Predicting the Morphologies of Confined Copolymer/Nanoparticle Mixtures

Jae Youn Lee, Zhenyu Shou, and Anna C. Balazs*

Chemical and Petroleum Engineering Department, University of Pittsburgh, Pittsburgh, Pennsylvania 15261

Received June 5, 2003; Revised Manuscript Received August 6, 2003

ABSTRACT: To isolate the factors that control the structure of nanocomposite thin films, we develop a computational model and scaling theory to investigate the behavior of diblock/nanoparticle mixtures that are confined between two hard walls. We find that in such restricted geometries a polymer-induced depletion attraction drives the particles to these walls. If the particles are chemically distinct from the walls, they will effectively modify the chemical nature of these substrates. This change in chemistry, in turn, affects the polymer−wall interactions and consequently the structure of the film. We illustrate this point by considering mixtures of particles and symmetric diblocks and show that the confining walls can be exploited to promote the self-assembly of the system into particle nanowires that extend throughout the films and are separated by nanoscale stripes of polymer domains. Such films constitute vital components in the fabrication of nanoscale devices. Furthermore, the results point to a novel technique for modifying the chemical nature of coatings and films entirely through self-assembly. Since this technique relies on entropic effects, it constitutes a fairly robust method that can be applied more generally than approaches that rely primarily on chemistry-specific enthalpic effects.

Introduction

Thin films that contain layers of both organic polymers and inorganic particles can exhibit remarkable mechanical properties.[1] For example, consider the unique strength of a mollusk's shell, which consists of alternating layers of biopolymers and inorganic platelets. The inorganic components impart stiffness, and the polymeric layers prevent the material from being brittle. Thus, the composite integrates the desirable features of each of the constituents. Recently, there has been considerable interest in adopting this layered organic/inorganic structural motif to create multifunctional coatings that combine the unique optical, electrical, and magnetic properties of semiconductor or metal nanoparticles with the processability and flexibility of polymers.[2−4] In effect, the interleafing of layers of polymers and inorganic particles provides new opportunities for tailoring the properties of thin films. Experimental studies have in fact yielded multilayer polymer/nanoparticle films where the optical, magnetic, and electrooptical properties of the composite can be tailored by varying the size or chemical nature of the nanoparticles.[2] Furthermore, the flexibility and structural integrity provided by the intervening polymer layers facilitate the incorporation of these thin films into various devices and microsystems.[3]

In this paper, we use both a computational approach and scaling theory to investigate how the presence of hard, confining walls can be exploited to promote the facile formation of spatially organized polymer/nanoparticle thin films. In previous studies of copolymer melts confined between two surfaces,[5] researchers have shown that the polymer−wall interactions can be harnessed to tailor the orientation and overall morphology of the films. However, the concept of forming spatially ordered composite films by confining copolymer/particle mixtures between two hard surfaces is relatively unexplored. To the best of our knowledge, there have been no systematic experimental or theoretical studies into the self-assembly and equilibrium structures of particle-filled copolymer films in such confined geometries.

To examine such systems, we extend our "SCF/DFT" model for the bulk equilibrium structure of blends of copolymers and nanoparticles[6−11] to polymer/particle mixtures confined between two hard surfaces. Our model for the bulk system combines a self-consistent-field theory (SCFT) for diblock copolymers and a density functional theory (DFT) for particles to yield a "SCF/DFT" model for nanocomposites. We now build on this formalism to model the morphology of thin films of particle-filled diblock copolymers.

In addition, we develop a scaling theory in the strong segregation limit that allows us to determine the effect of the particles on the behavior of the confined diblocks. Through the scaling theory, we can validate the predictions from the SCF/DFT calculations and show that the observed effects are sufficiently robust that they can be found in both the strong and intermediate segregation limits of the diblock melts (i.e., both low and intermediate temperatures).

As we show below, the confined diblock/particle mixtures exhibit a rich phase behavior. This behavior results from the complex interplay of entropic and enthalpic interactions that occur among all the components in such restricted geometries. For example, because of entropic interactions, the polymers induce a "depletion attraction" between the particles and walls. Localized at the walls, these particles modify the enthalpic interactions between the polymers and substrates and consequently can control the morphology of the layers. Through these studies, we isolate a case where the system self-assembles into particle-decorated lamellar layers that are oriented perpendicular to the surfaces. The removal of the surface layers (by microtoming, for example) reveals an ordered nanoscale pattern, with alternating polymeric and metallic stripes,

* Corresponding author. E-mail: balazs1@engr.pitt.edu.

10.1021/ma034765d CCC: $25.00
Published on Web 09/09/2003

or "nanowires", which extend throughout the film. These films constitute vital components, as the miniaturization of devices is driving the need for feature sizes on the nanometer length scale. More generally, the results reveal a robust method for promoting the spontaneous ordering of the components into nanostructured organic/inorganic thin films.

Below, we first describe both the computational and scaling models and then discuss the effects of the solid additives on the behavior of the confined films.

The Models

SCF/DFT Approach. We consider a mixture of AB diblocks and hard cubic particles;[12−14] the edge of each cube is of length σ. This mixture is confined between two parallel plates, separated by a distance Δ. The total volume of the system is V; the volume fraction of particles in this system is ϕ_p, and that of the diblocks is $(1 - \phi_p)$. Each diblock is modeled as a flexible Gaussian chain consisting of N segments of segment volume ρ_0^{-1} and statistical segment length a. The fraction of A type monomers along a chain is denoted by f. Here, we focus on symmetric diblocks by setting $f = 0.5$. We also fix $\bar{N} = 1000$, where $\bar{N} = \rho_0^2 a^6 N$ is the invariant polymerization index. Since we are interested in the microphase-separated regime, we set $\chi_{AB}N = 20$, where χ_{AB} is the Flory−Huggins interaction parameter between the A and B blocks.

The $\varphi_i(\mathbf{r})$ are the local volume fractions of species i. The confining walls are located at $z = 0$ and $z = \Delta$, at which points the concentration of the mixture vanishes. To avoid numerical difficulties arising from the boundary condition, we take the incompressibility constraint to be $\varphi_A(\mathbf{r}) + \varphi_B(\mathbf{r}) + \varphi_p(\mathbf{r}) = \Phi_0(\mathbf{r})$ such that the concentration of the mixture decays smoothly inside the region of width ϵ immediately next to the confining walls and set

$$\begin{aligned}\Phi_0(\mathbf{r}) &= \frac{1 - \cos(\pi z/\epsilon)}{2} \quad 0 \le z \le \epsilon \\ &= 1 \quad \epsilon \le z \le \Delta - \epsilon \\ &= \frac{1 - \cos(\pi(\Delta - z)/\epsilon)}{2} \quad \Delta - \epsilon \le z \le \Delta \end{aligned} \tag{1}$$

where ϵ is chosen such that $\epsilon \ll \Delta$. Here, we take $\epsilon = 0.15R_0$, which is the value used by Matsen for the case of confined diblocks.[15] We have tested smaller ϵ ($0.05R_0 < \epsilon < 0.15R_0$) and found that within this range, results do not depend on the specific value of ϵ.

The free energy of the system is adapted from our SCF/DFT model.[6−11] In SCF theory, pairwise interactions between differing segments are replaced by the interaction of each segment with the average field created by the other segments. Here, we let $w_A(\mathbf{r})$ denote the value of the mean field felt by A segments at $\mathbf{r}$, $w_B(\mathbf{r})$ the field for B segments, and $w_p(\mathbf{r})$ the field for particles. Using this approach,[6−11] the free energy of the system is given by $F = F_d + F_p + F_e$. (Note that $F \equiv NF/\rho_0 k_B T V$ and is a dimensionless free energy.) The diblock entropic free energy is described by F_d as follows:

$$F_d = (1 - \phi_p)\ln[V(1 - \phi_p)/Q_d] - (1/V)\int d\mathbf{r}\,[w_A(\mathbf{r})\,\varphi_A(\mathbf{r}) + w_B(\mathbf{r})\,\varphi_B(\mathbf{r})] \tag{2}$$

where Q_d is the partition function of a single diblock subject to the fields $w_A(\mathbf{r})$ and $w_B(\mathbf{r})$. F_p accounts for particle entropic contributions to the free energy and the excess free energy due to steric interactions between the particles and has the form

$$F_p = -\frac{\phi_p}{\alpha}\ln\left(\frac{Q_p\alpha}{V\phi_p}\right) - (1/V)\int d\mathbf{r}\,[w_p(\mathbf{r})\,\rho_p(\mathbf{r}) - \rho_p(\mathbf{r})\,\Psi_{FMT}(\varphi_p(\mathbf{r}))] \tag{3}$$

Here Q_p is the partition function for a single particle, α is the diblock-to-particle volume ratio, ρ_p is the particle center distribution, and $\Psi_{FMT}(\varphi_p(\mathbf{r}))$ is the steric energy contribution. To describe these steric interactions, we adopt density functional theory; in particular, we adopt the fundamental measure theory (FMT) for parallel hard cubes.[16] We introduce this density functional term so that the model can describe not only homogeneous (liquid) but also inhomogeneous (crystalline) distributions of particles. We chose the FMT formulation of DFT because it can be readily extended to various parallelepipeds,[14] and thus, we can ultimately examine how the aspect ratio of the particles affects the structure of the films.

The term F_e details the enthalpic interactions, which include block−block, block−particle, block−surface, and particle−surface interactions and is

$$F_e = (1/V)\int d\mathbf{r}\,[\chi_{AB}N\varphi_A(\mathbf{r})\,\varphi_B(\mathbf{r}) + \chi_{AP}N\varphi_A(\mathbf{r})\,\varphi_p(\mathbf{r}) + \chi_{BP}N\varphi_B(\mathbf{r})\,\varphi_p(\mathbf{r})] - (1/V)\int d\mathbf{r}\,[H_A(\mathbf{r})\,N\varphi_A(\mathbf{r}) + H_B(\mathbf{r})\,N\varphi_B(\mathbf{r}) + H_p(\mathbf{r})\,N\varphi_p(\mathbf{r})] \tag{4}$$

where χ_{ij} is the Flory−Huggins parameter between species i and j, and $H_i(\mathbf{r})$ describes the surface field for either diblocks or particles. The functional form of the surface field is

$$\begin{aligned}H_i(\mathbf{r}) &= \infty \quad 0 \le z \le \delta \\ &= \frac{\Lambda_{iw}}{\epsilon}(1 + \cos(\pi(z - \delta)/\epsilon)) \quad \delta \le z \le \epsilon + \delta \\ &= 0 \quad \epsilon + \delta \le z \le \Delta - \epsilon - \delta \\ &= \frac{\Lambda_{iw}}{\epsilon}(1 + \cos(\pi(\Delta - \delta - z)/\epsilon)) \quad \Delta - \epsilon - \delta \le z \le \Delta - \delta \\ &= \infty \quad \Delta - \delta \le z \le \Delta \end{aligned} \tag{5}$$

Here, $\delta = 0$ for diblocks and $\delta = \sigma$ for particles. Λ_{iw} represents the strength of the interaction between the surface and species i; a negative value of Λ_{iw} corresponds to a repulsive interaction, while a positive value indicates an attractive interaction.[15]

The complete free energy expression is now minimized to obtain the possible equilibrium structures. For this process, we employ the combinatorial screening method of Drolet and Fredrickson[17] to locate the saddle points in the free energy surface. The calculations are carried out in two dimensions (involving the x and z directions), and we assume translational invariance along y. In addition, we minimize the free energy with respect to the simulation box size in the lateral (x) direction.[18]

Scaling Theory. Our scaling theory is based on a strong segregation model developed by Turner[19] and Walton et al.[20] to describe the behavior of pure, symmetric diblocks that are confined between two parallel plates. The model is also based on our previous scaling

analysis for the bulk behavior of nanoparticle/diblock mixtures.[13] In the case of thin films, the confined lamellar layers can orient either parallel or perpendicular to the plates, depending on the block-surface interactions.[5,15,20,21] Here, we derive a free energy expression for diblock/particle mixtures that takes into account these two possible orientations.

The mixture contains a volume fraction ϕ_p of spherical particles of radius R and a volume fraction $(1 - \phi_p)$ of symmetric AB diblocks, where the degree of polymerization of the A and B blocks is given by $N/2$. The mixture is confined between two chemically identical, parallel plates that are separated by a distance Δ. The interaction between species i and j is characterized by the interfacial tension γ_{ij} (which is dimensionless, in units of k_BT/a^2).[19] We assume a preferential block−surface interaction such that $\gamma_{AS} < \gamma_{BS}$, and a neutral block−particle interaction specified by $\gamma_{Ap} = \gamma_{Bp} \equiv \gamma_{dp}$ where the subscripts A, B, d, p, and S denote A and B blocks, the diblock, particles, and surfaces, respectively. The interactions between the A and B blocks and the particles and surfaces are described by γ_{AB} and γ_{PS}, respectively.

The width of the film, Δ, is divided into three regions. The top and bottom surface layers are assumed to have a width of $2R$, allowing this region to accommodate a single layer of particles. The width of the middle layer is taken to be $(\Delta - 4R)$. The volume fraction of particles is allowed to vary within the entire film; however, the particle volume fraction is assumed to be uniform within each of these three regions. We define $\phi_t = \phi_b \equiv \phi_S$ as the local volume fraction of particles in the respective top and bottom surface layers. In addition, ϕ_m is the local particle volume fraction in the middle layer. We assume that the minimum volume fraction of particles in the surface layers is equal to ϕ_p; this situation would correspond to a uniform distribution of particles throughout the entire film (not just within each layer). In other words, within the top or bottom layers, we have $\phi_{min} \le \phi_S \le \phi_{max}$, where $\phi_{min} = \phi_p$ and $\phi_{max} = \phi_p/(4R/\Delta)$. The local particle volume fraction in the middle layer is given by $\phi_m = \Delta(\phi_p - \phi_S\,(4R/\Delta))/(\Delta - 4R)$. When $\phi_S = \phi_{max}$, all the particle are located in the surface layers, and there are no particles in middle section. We note that ϕ_{max} is not allowed to exceed the volume fraction that corresponds to the close packing fraction of spheres.

We now describe the free energy density of the system ($g \equiv g/Vk_BT$ and a, the segment length, is set to 1). First, the bulk contribution from the diblock melt is

$$g_{d/bulk} = \frac{1 - \phi_p}{N}\left[\frac{3L^2}{8N} + \frac{2N\gamma_{AB}}{L}\right] \tag{6}$$

where L is the diblock period. For the surface-perpendicular orientation, $L = L^*$, where L^* is the equilibrium diblock period. In addition, the translational entropy of the diblock is

$$g_{d/trans} = \frac{1 - \phi_p}{N}\ln(1 - \phi_p) \tag{7}$$

The contributions from the particles can be divided into three components—the translational entropy of the particles, the steric energy between the particles, and the loss of the conformational entropy of the chains due to particles—and are given by

$$g_{p/trans} = \frac{\phi_t}{v_p}(2R/\Delta)\ln\phi_t + \frac{\phi_b}{v_p}(2R/\Delta)\ln\phi_b + \frac{\phi_m}{v_p}\left(\frac{\Delta - 4R}{\Delta}\right)\ln\phi_m \tag{8}$$

$$g_{p/steric} = \frac{\phi_t}{v_p}(2R/\Delta)\Psi_{cs}(\phi_t) + \frac{\phi_b}{v_p}(2R/\Delta)\Psi_{cs}(\phi_b) + \frac{\phi_m}{v_p}\left(\frac{\Delta - 4R}{\Delta}\right)\Psi_{cs}(\phi_m) \tag{9}$$

$$g_{p/conf} = \frac{\phi_t}{v_p}(2R/\Delta)(1 - \phi_t)\frac{R^2}{4Na_0^2} + \frac{\phi_b}{v_p}(2R/\Delta)(1 - \phi_b)\frac{R^2}{4Na_0^2} + \frac{\phi_m}{v_p}\left(\frac{\Delta - 4R}{\Delta}\right)(1 - \phi_m)\frac{R^2}{4Na_0^2} \tag{10}$$

In the above equations, v_p is the volume of the spherical particle. These expressions are based on our previously derived scaling model for the bulk behavior of diblock/particle mixtures,[13] and we refer the reader to ref 13 for a more detailed description of the theory. In eq 9, $\Psi_{CS}(\psi) = (4\psi - 3\psi^2)/(1 - \psi)^2$ is the Carnahan−Starling equation for hard spheres.[22] In eq 10, $a_0 = 1/\sqrt{6}$. The terms proportional to $R^2/4Na_0^2$ in eq 10 describe the stretching in the transverse directions that the chains must undergo in order to get around the particles;[13,23] there is a contribution from each region of the film. Note that when $\phi_i = 0$ (where i = t, b, and m), eq 10 goes to 0, and when $\phi_i = 1$, this term also goes to zero; in between these limits, the term scales as $(1 - \phi_i)$.

To complete the free energy expression, we now must include the enthalpic contribution between different species. First, the block−particle interaction energy is given by

$$g_{dp} = \phi_t(1 - \phi_t)(2R/\Delta)\gamma_{dp}\Sigma_p + \phi_m(1 - \phi_m)\left(\frac{\Delta - 4R}{\Delta}\right)\gamma_{dp}\Sigma_p + \phi_b(1 - \phi_b)(2R/\Delta)\gamma_{dp}\Sigma_p \tag{11}$$

where $\Sigma_p = 0.5/R$ is the number of surface contacts for each particle.[13] We normalize the ratio such that for $R = 0.5$ the expression reduces to the expression for diblocks in a solvent. Second, the particle−surface interaction energy is given by

$$g_{pS} = \frac{\phi_t\gamma_{pS}}{\Delta} + \frac{\phi_b\gamma_{pS}}{\Delta} = 2\frac{\phi_S\gamma_{pS}}{\Delta} \tag{12}$$

For the block−surface interactions, we must consider the parallel and perpendicular orientations separately. For the parallel case, we assume the A block is located next to the surfaces since we set $\gamma_{AS} < \gamma_{BS}$, and the energy is given by

$$g_{dS_{||}} = 2\frac{\gamma_{AS}}{\Delta}(1 - \phi_S) \tag{13}$$

For the perpendicular orientation, the energy is given by

$$g_{dS_\perp} = 2f\frac{\gamma_{AS}}{\Delta}(1-\phi_S) + 2(1-f)\frac{\gamma_{BS}}{\Delta}(1-\phi_S) \quad (14)$$

where f is the fraction of A monomers within a chain. For the symmetric diblocks studied here, $f = 0.5$.

The sum of the above terms, g_{tot}, yields the free energy density for our system. In carrying out these calculations, we fix ϕ_p, the γ_{ij}, and R and minimize g_{tot} with respect to ϕ_S. We evaluate the energy expressions for both the parallel and perpendicular cases. The orientation that has the lower free energy is deemed to be the equilibrium structure. In addition, we calculate phase maps for the system as a function of particle size, R. These plots are described below.

Results and Discussion

SCF/DFT Studies. In the absence of filler particles, a melt of microphase-separated, symmetric AB diblocks confined between two surfaces forms lamellar layers, with stripes oriented either parallel or perpendicular to the walls.[5,15,20,21,24] If the walls have a preferential interaction with one of the blocks, this orientation depends on the surface separation, Δ (however, for relatively strong preferential interactions, the confined copolymers will generally yield the parallel structure).[5,15,20,21] If, on the other hand, the walls are nonselective and thus have a neutral interaction with both blocks, the film exhibits the perpendicular orientation for all Δ.[5,15,21]

To test our model and establish a basis for comparison, we first examine the behavior of the pure diblock melt confined between two walls. To simulate this particle-free case, we set $\phi_p = 0$ in the above equations. We begin by considering the typical experimental case where the confining walls have a preferential interaction with one of the blocks of the diblock. Here, we set $\Lambda_{AW}N = 0.2$ and $\Lambda_{BW}N = -0.2$ so that each wall has an attractive interaction with the A block and a repulsive interaction with B. For each value of the surface separation, Δ, we undertake two separate calculations, with either the surface-parallel or surface-perpendicular configuration as the initial condition. We then compare the final free energy F and take the system with the lower F as the equilibrium structure. Figure 1 shows a plot of the equilibrium lamellar orientation vs surface separation. The vertical axis of the plot is the excess free energy due to the surface, $(F - F_b)\Delta$, where F_b is the bulk free energy of the symmetric diblock melt. The horizontal axis of the plot is in terms of Δ/D_b, where D_b is the bulk lamellar spacing. The results agree with previous theoretical calculations,[5,15,20,21] showing that the parallel orientation has the lower free energy at surface separations close to and at integer multiples (n) of the bulk lamellar spacing, i.e., at $\Delta/D_b = n$. When one of the substrates is removed in the case of such surface-parallel structures, the underlying film reveals a uniform layer of A or B polymers, which does not yield a significant advantage for technological applications.

With the above parameters held fixed, we now introduce a volume fraction $\phi_p = 0.1$ of neutral (nonselective) particles characterized by $\chi_{AP}N = \chi_{BP}N = 5$ and $\sigma = 0.3R_0$, where R_0 is the root-mean-squared end-to-end distance of the bulk diblock chain. The particle−wall interaction is repulsive at $\Lambda_{PW}N = -0.2$ and is approximately of the same magnitude as the particle−polymer interactions. Figure 2 shows the excess free energy vs surface separation for both the perpendicular and parallel morphologies of the filled diblocks when $\phi_p = 0.1$; note that D_b now refers to the bulk lamellar period for the filled system. The perpendicular structure has the lower free energy for all surface separations despite the preferential block−wall interactions.

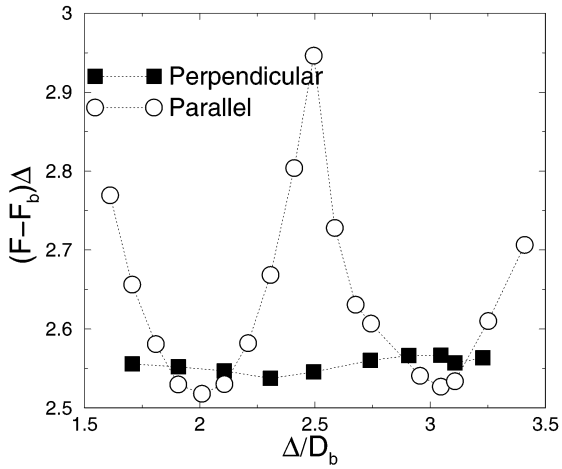

Figure 1. Excess free energy for pure diblock films as a function of Δ/D_b for the parallel (open circles) and perpendicular (filled squares) orientations. F_b is the bulk free energy, and D_b is the bulk lamellar spacing. Here, $\bar{N} = 1000$, $\chi_{AB}N = 20$, $\Lambda_{AW}N = 0.2$, $\Lambda_{BW}N = -0.2$, and $f = 0.5$.

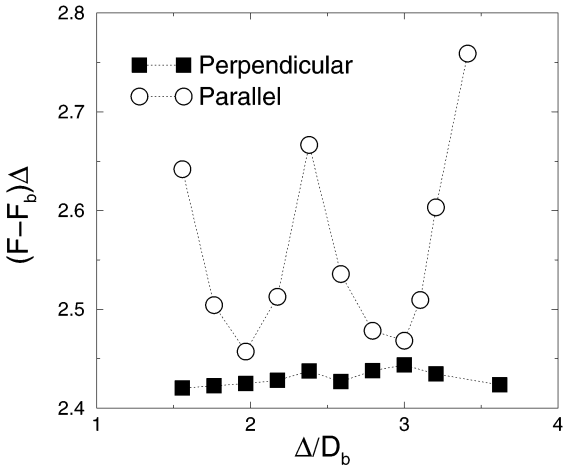

Figure 2. Excess free energy for diblock/nanoparticle composite films as a function of Δ/D_b for the parallel (circles) and perpendicular (filled squares) orientations. F_b is the bulk free energy, and D_b is the bulk lamellar spacing for the particle-filled systems. Here $\bar{N} = 1000$, $\chi_{AB}N = 20$, $\Lambda_{Aw}N = 0.2$, $\Lambda_{BW}N = -0.2$, $f = 0.5$, $\phi_p = 0.1$, $\sigma = 0.3R_0$, and $\chi_{AP}N = \chi_{BP}N = 5$.

To understand this behavior, we examine the volume fraction profiles for the particle-filled perpendicular and parallel structures at $\Delta/D_b = 2$, as shown in Figure 3. We first focus on the lower free energy perpendicular film in Figure 3a,b. The profiles show that the particles are localized at the surfaces and at the A/B interfaces, where they extend vertically through the film. Note that, in this case, the removal of the surface layers reveals a periodic array of particle "nanowires" that are separated by the nanoscale polymer domains, yielding a vital material for nanodevice fabrication. For a more detailed image of the particle distribution within this film, we turn to Figure 4, which shows a surface plot of the local volume fraction, φ_P. For this value of Δ,

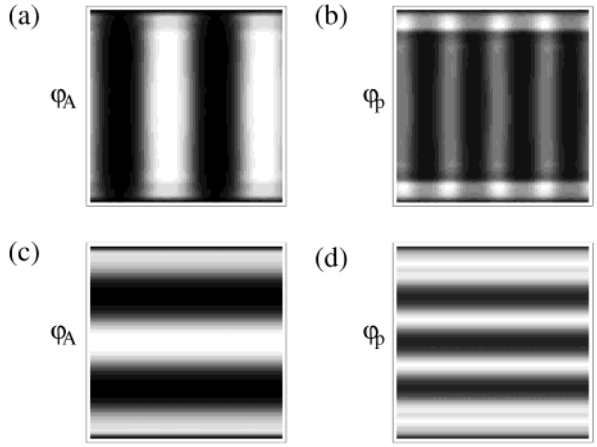

Figure 3. Density contour plots for a diblock/nanoparticle film of width $\Delta = 2D_b$. Other parameters are identical to the ones shown in Figure 2. Light regions indicate the presence of a species and dark regions mark the absence of a species. Images (a) and (b) depict the local volume fraction of the *A* block, φ_A, and the particles, φ_p, respectively, for the perpendicular orientation, which exhibits the lower free energy. Images (c) and (d) show these local volume fractions for the parallel structure.

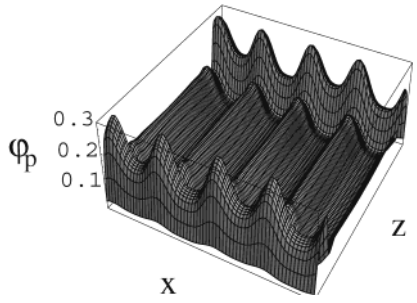

Figure 4. Surface plot of the particle distribution for the perpendicular system shown in Figure 3.

approximately 65% of the particles are confined at the A/B interface, while 35% are localized at the hard walls. (The exact numbers will depend on the value of Δ; as expected, greater surface separations yield smaller values at the hard surfaces.) Since the surface region occupies roughly 18% of the volume at this Δ, a uniform particle distribution would have 18% of the fillers localized in this surface region. Qualitatively similar results are also seen at $\phi_p = 0.15$.

The reason why the system assumes this particle-decorated perpendicular morphology arises from an interplay of enthalpic and entropic effects. In particular, the neutral particles are driven to the A/B boundary by enthalpic effects; localized at the interface, the fillers effectively reduce the interfacial tension between the A and B domains.[8] On the other hand, the particles are driven to the surfaces primarily by entropic interactions. (The particle−block repulsion also promotes the expulsion of the particles.) In such highly confined geometries, the conformational entropy of the chains is greater when a fraction of the particles are "pushed" to the surfaces than when they are all confined within the bulk of the film. To test this assertion, we compared the conformational entropy term for the A and B blocks for the self-assembled structure in Figure 4 with an artificially "biased" structure where all the particles are constrained to remain localized at the A/B interface. Table 1 shows that the loss in conformational entropy of the both the A and B blocks is less in the case where a

Table 1. Comparison of Contributions to the Total Free Energy, *F*, for the Self-Assembled Perpendicular Film (Figure 3a,b) and a Perpendicular Film in Which the Particles Are Constrained To Remain at the A/B Interfaces[a]

	self-assembled perpendicular	particle fixed perpendicular
F	4.279	4.360
S_A	1.192	1.284
S_B	1.136	1.224
S_P	−0.183	−0.217
F_e	1.968	1.953

[a] S_A (S_B) is the loss in conformational entropy of the A (B) blocks (as obtained from eq 2), S_P is the contribution from the translational entropy of the particles (the first term in eq 3), and F_e is the contribution from the enthalpic interactions (eq 4). (The particle−wall interaction is repulsive, yielding a higher F_e for the self-assembled case.)

Table 2. Comparison of Contributions to the Total Free Energy, *F*, for the Self-Assembled Perpendicular Film (Figure 3a,b) and a Parallel Film (Figure 3c,d)

	Perpendicular	Parallel
F	4.279	4.287
S_A	1.192	1.494
S_B	1.136	0.831
S_P	-0.183	-0.209
F_e	1.968	2.050

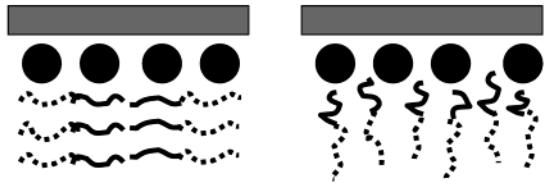

[a] S_A (S_B) is the loss in conformational entropy of the A (B) blocks, S_P is the contribution from the translational entropy of the particles, and F_e is the contribution from the enthalpic interactions. The cartoons show the arrangement of the particles in the perpendicular (left) and parallel (right) configurations. Since the chains in the parallel phase lie perpendicular to the surface, the conformations of the A blocks are highly constrained by the particles at the wall.

fraction of the particles are localized at the surface. In other words, to gain conformational entropy, the confined polymers induce an effective attraction (i.e., a "depletion" attraction) between the neutral particles and surfaces.

Once at the surface, the layer of nonselective particles modifies the chemical nature of the selective surface. In essence, the A blocks now experience more neutral or less attractive walls. In the presence of the neutral (or weakly attractive) substrates, the surface-perpendicular diblock morphology is energetically more favorable[5,15,21,24] than the surface-parallel structure. The later behavior can explain the findings in Figure 2, where the particle-filled perpendicular structure has the lower free energy.

A comparison of the different free energy contributions to the parallel and perpendicular structures in Figure 3 is also useful in understanding why the perpendicular structure is preferred. This breakdown is given in Table 2. A significant difference between the two cases arises from the conformational entropy contribution of the A blocks. This can be understood by referring to Figure 3c,d and the cartoon in Table 2. The density plots again reveal that the polymer-mediated

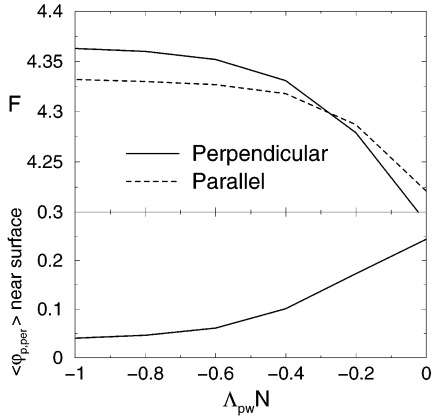

Figure 5. Dependence of morphologies on particle-surface interactions. In the upper panel, free energy for the perpendicular (solid curve) and parallel (dashed curve) morphologies is plotted against $\Lambda_{PW}N$. Here, $N = 1000$, $\chi_{AB}N = 20$, $\Lambda_{AW}N = 0.2$, $\Lambda_{BW}N = -0.2$, $f = 0.5$, $\phi_p = 0.1$, $\sigma = 0.3R_0$, $\chi_{AP}N = \chi_{BP}N = 5$. In the lower panel, the volume fraction of particles averaged over the surface region is plotted against $\Lambda_{PW}N$.

depletion attraction pushes a fraction of the particles to the wall (and enthalpic interactions drive the particles to the A/B interfaces). The fraction of particles at the surface is comparable in both the parallel and perpendicular scenarios. But as the cartoon indicates, in the surface-parallel structure, the A chains lie orthogonal to the particle layer and are highly compressed by the presence of these fillers. Consequently, they exhibit a higher loss in conformational entropy than in the surface-perpendicular case, where the A chains lie along the surface.

In the above calculations, the particle−wall interaction was fixed at $\Lambda_{PW}N = -0.2$, indicating a weakly repulsive interaction. The polymer induced depletion attraction offsets this weak particle−wall repulsion and leads to a localization of the particles at the wall. It is of particular interest to determine how the magnitude of the particle−wall interaction affects the equilibrium orientation of the film. Figure 5 reveals that as this repulsion is increased beyond $\Lambda_{PW}N = -0.4$, the parallel morphology has the lower free energy because the volume fraction of particles at the walls has decreased beyond a critical amount. When the volume fraction of particles at the wall is less than approximately 10%, there are not enough particles to alter the effective polymer−wall interactions.

In the above studies, the total volume fraction of particles, ϕ_p, was held fixed at 0.1 (comparable results were also found for $\phi_p = 0.15$). It is also of significant interest to estimate a lower bound for ϕ_p at which the surface-perpendicular structures are more energetically favorable than the surface-parallel structures. Figure 6 shows the free energy vs surface separation for different values of ϕ_p. As can be seen, already at $\phi_p = 0.05$, the perpendicular structure has the lower free energy at all surface separations. While this seems a relatively low volume fraction to have such a dramatic effect, it is worth noting that Wiesner et al.[25] recently showed that when a comparable amount of nanoparticles was added to the bulk diblock melt, the fillers significantly suppressed the order−disorder transition temperature. Thus, it is conceivable that such a small volume fraction of particles would have a significant influence in this more constrained, thin film environment.

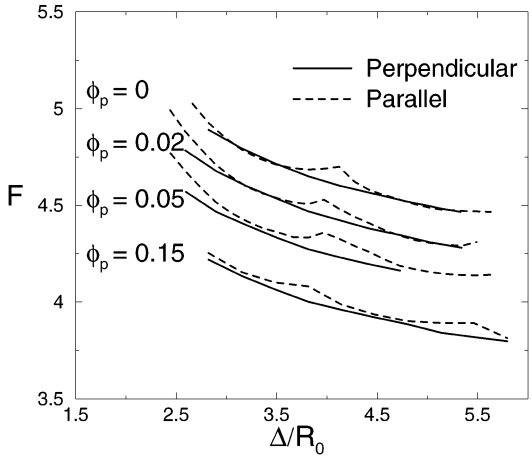

Figure 6. Dependence of morphologies on the volume fraction of particles. Free energy of the parallel (dashed curve) and perpendicular (solid curve) structures as a function of surface separation for systems containing various volume fractions of particles. (Δ is divided by R_0 to make this value dimensionless.) For systems containing more than 5% particles, the free energy for the perpendicular structure is always lower.

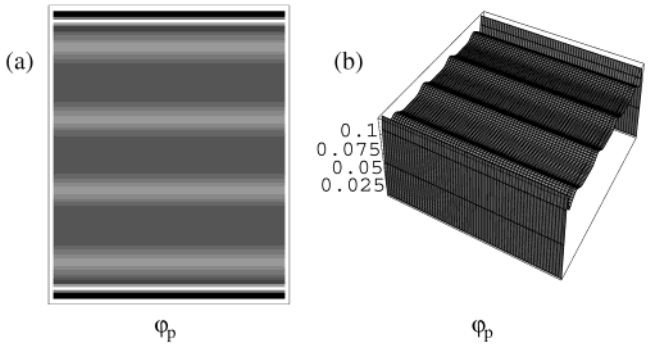

Figure 7. Particle distribution for the diblock/nanoparticle composite film where $N = 1000$, $\chi_{AB}N = 20$, $\Lambda_{AW}N = 0.2$, $\Lambda_{BW}N = -0.2$, $f = 0.5$, $\phi_p = 0.1$, $\sigma = 0.1R_0$, $\chi_{AP}N = \chi_{BP}N = 5$, $\Lambda_{PW}N = -0.2$, and $\Delta = 2D_b$. (a) shows the density plot, while (b) shows the surface plot of the local particle volume fraction. Compared to the larger particle case for the same set of parameters (Figures 3 and 4), the smaller particles distribute more uniformly throughout the entire film. Consequently, the parallel structure has the lower free energy.

In bulk systems, we previously compared the behavior of smaller and larger neutral nanoparticles[8] and found that the smaller species are more uniformly distributed throughout the copolymer matrix than the bigger ones because the smaller particles exhibit greater translational entropy. This observation has important consequences in the case of the confined thin films. If the particle size is reduced to $\sigma = 0.1R_0$, the particles are more extensively spread throughout the film and are less localized at the surface (see Figure 7) than for the comparable $\sigma = 0.3R_0$ example (see Figures 3 and 4). Polymers do not lose as much conformational entropy in stretching around the smaller particles as they do in extending around the larger ones. Consequently, there is less of a polymer-induced depletion attraction between the smaller fillers and the confining walls. This, in turn, affects the orientation of the film; with fewer neutral particles at the surface, there are not enough of these additives to effectively modify the walls, and the equilibrium structure for this system is the surface-parallel structure in Figure 7.

Having shown that *nonselective* nanoparticles can alter the relative orientation of the film when the

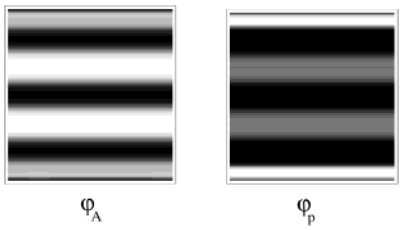

Figure 8. Structure of diblock/nanoparticle mixture that contains selective particles ($\chi_{Ap}N = 0$, $\chi_{Bp}N = 20$) and is confined between neutral walls ($\Lambda_{AW}N = \Lambda_{BW}N = 0$). The width of the film is $\Delta = 2.5D_b$. Here, $N = 1000$, $\chi_{AB}N = 20$, $f = 0.5$, $\phi_p = 0.1$, $\sigma = 0.3R_0$, and $\Lambda_{PW}N = 0$. The system exhibits a parallel morphology even at this noninteger surface separation.

diblocks are confined between *selective* walls, we now focus on another limit to show the substantial effect of these fillers. In particular, we now introduce *selective* particles and *nonselective* surfaces. Here, we focus on a smaller range of parameters and surface separations than considered above since our aim is to indicate a general trend, rather than to explore the phase space.

As noted at the beginning of this section, in the presence of nonselective (neutral) walls, the pure, symmetric diblock system forms surface-perpendicular lamellae. To model the presence of the nonselective walls, we set $\Lambda_{dW}N = 0$. By setting $\chi_{AP}N = 0$ and $\chi_{BP}N = 20$, we introduce a preferential affinity between the particles and the A blocks. We also set $\Lambda_{pW}N = 0$. Our hypothesis is that the particles will be driven to the walls by the entropic effects described above (since $\Lambda_{dW}N = \Lambda_{pW}N = 0$, enthaplic effects have been removed from the problem), and at the walls, these additives will make the surfaces more A-like. In the presence of the now more selective substrates, the system should adopt the parallel orientation, with the A layers being located at both the top and bottom of the film. As shown in Figure 8, this is in fact the lower free energy conformation, even at the noninteger value of $\Delta/D_b = 2.5$, where in the absence of particles the perpendicular orientation would be preferred.

The above SCF/DFT calculations indicate that the addition of the particles can be exploited to tailor the chemical nature of the confining surfaces and thereby control the morphology of the composite film. Below, we use our strong segregation scaling theory for the diblock/nanoparticle films to test these predictions. In this scaling theory, we assume that the particles are spherical in shape; as we show below, the general predictions are equally valid for cubic and spherical particles.

Scaling Theory Calculations. Our aim in carrying out the scaling theory calculations is not to make a direct numerical comparison with the SCF/DFT results; such a comparison would be inappropriate since our SCF/DFT calculations were carried out in the intermediate segregation region, while the scaling theory is appropriate for the strong segregation regime. Furthermore, the SCF/DFT model provides greater structural detail than the scaling model, where the particles are assumed to be uniformly distributed throughout the surface and middle layers. Thus, the inherent assumptions in the two models are somewhat different. Nor is our aim to carry out an extensive exploration of the phase space. Rather, our goal is to use an additional, distinct model to focus on the case of the neutral particles and validate the general prediction that these particles are expelled to the surfaces and, once at the surfaces, stabilize the perpendicular orientation relative

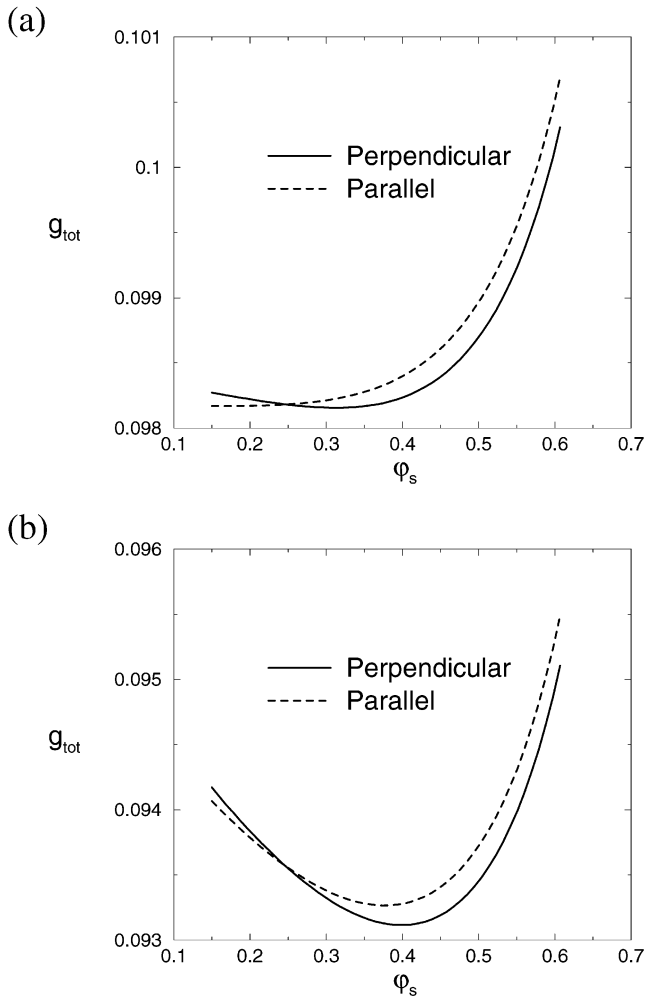

Figure 9. Effect of particles localized in the surface regions. Free energies of the perpendicular (solid curve) and parallel (dashed curve) orientations are plotted against φ_s, the local volume fraction of particles in the surface region. The curves are calculated using the strong segregation scaling theory (SST). Here, $N = 100$, $\phi_p = 0.15$, $R = 4$, $\gamma_{AB} = 1$, $\gamma_{As} = 0.3$, $\gamma_{Bs} = 0.37$. In (a), $\gamma_{dp} = \gamma_{ps} = 0.3$ and in (b) $\gamma_{dp} = \gamma_{ps} = 0.1$.

to the parallel structure. In this manner, we can show the findings are not model-dependent and that the phenomenon is sufficiently robust that it occurs in both the intermediate segregation regime (intermediate temperatures) captured by the SCF/DFT model and strong segregation regime (low temperatures) captured by the scaling theory.

In the ensuing calculations described below, we fix $N = 100$ and $\phi_p = 0.15$. Figure 9a shows the free energy vs ϕ_S for a confined mixture where $R = 4$, $\gamma_{AB} = 1$, $\gamma_{AS} = 0.3$, $\gamma_{BS} = 0.37$, and $\gamma_{dp} = \gamma_{pS} = 0.3$. Figure 9b shows the comparable curve for $\gamma_{dp} = \gamma_{pS} = 0.1$. Through this choice of parameters, we model a system where the walls have a preferential affinity for the A blocks, the particles are nonselective (neutral) with respect the A and B phases, and the unfavorable particle−block and particle−wall interactions are comparable.[26] Thus, the system is analogous to cases studied above with the SCF/DFT approach. The value of $\Delta = 1.1L^*n$, where L^* is the equilibrium lamellar spacing for the pure diblock system[27] and n is the number of lamellar periods. Here, $n = 2$ (which corresponds to two layers of A and two layers of B).

We first consider the lower plot, Figure 9b, where the surface tension between the particles and walls is

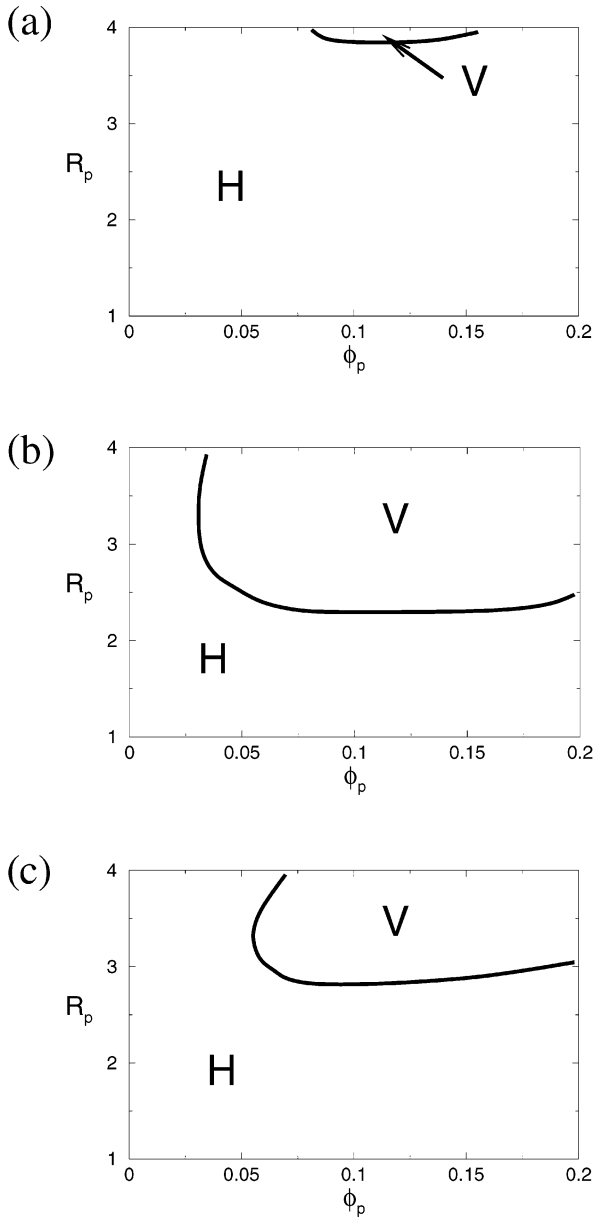

Figure 10. Phase map for the composite film as a function of particle size, R_p, and volume fraction of particles, ϕ_p, as calculated using the SST. The region where the perpendicular morphology is the equilibrium structure is labeled by a V (for vertical), and the region where the parallel morphology is the equilibrium structure is marked by H (for horizontal). Here, $N = 100$, $\phi_p = 0.15$, $R = 4$, $\gamma_{AB} = 1$. In (a), $\gamma_{As} = 0.3$, $\gamma_{Bs} = 0.37$, and $\gamma_{dp} = \gamma_{ps} = 0.3$; in (b), $\gamma_{As} = 0.3$, $\gamma_{Bs} = 0.37$, and $\gamma_{dp} = \gamma_{ps} = 0.1$; in (c), $\gamma_{As} = 0.5$ $\gamma_{Bs} = 0.58$ and $\gamma_{dp} = \gamma_{ps} = 0.3$.

relatively low. The curves illustrate two interesting features. First, it can be seen that free energy for both parallel and perpendicular morphologies is at a minimum when the particles are preferentially localized at the surfaces, rather than being uniformly distributed throughout the film (which corresponds to $\phi_S = 0.15$). The second important feature is that the perpendicular structure exhibits the lower free energy. In the absence of these particles at a surface separation of $1.1L^*n$, the parallel morphology would correspond to the equilibrium structure[5] (see Figure 10). But as we saw from the SCF/DFT results, the presence of the solid additives alters the preferable morphology from parallel to perpendicular. Thus, both the scaling theory and the SCF/DFT point to the same general trend: the particles localize at the walls and, as a result, modify the morphology of the confined layers.

We next consider the upper plot, Figure 9a, where the particle−wall surface tension is relatively higher. The perpendicular orientation with the particles localized at the surface still exhibits the globally lower free energy. It is interesting to note that, in the case of the parallel structure, a uniform distribution of particles has the lowest free energy for the possible parallel structures.

The scaling theory is a useful approach for generating phase maps that reveal the effect of particle size.[8] To test another prediction that emerged from the SCF/DFT model, we now use the scaling approach to determine how the particle size affects the relative orientation of the film. Figure 10a shows a phase map as a function of R and ϕ_p for $N = 100$, $\gamma_{AB} = 1$, $\gamma_{AS} = 0.3$, $\gamma_{BS} = 0.37$, and $\gamma_{dp} = \gamma_{pS} = 0.3$ at $\Delta = 1.1L^*n$, where $n = 2$. As can be seen, in the absence of particles, the parallel structure is the stable morphology. However, the figure reveals a distinct region for $R \approx 4$ and $0.05 < \phi_p < 0.20$ where the perpendicular morphology is the equilibrium structure. As we saw with the SCF/DFT calculations, we again see that the addition of relatively large neutral particles can be used to stabilize the perpendicular orientation.

Making the particle−surface interactions more favorable than the polymer−surface interactions can broaden the range in which the perpendicular structure is stabilized. Under these conditions, it is energetically more favorable for the particles than the polymers to be localized at the walls; at the walls, the neutral particles promote the creation of the perpendicular film. This behavior can be seen in Figure 10b, where the interfacial tension between the particles and surface is decreased ($\gamma_{pS} = \gamma_{dp} = 0.1$) relative to the fixed values for the polymers ($\gamma_{AS} = 0.3$, $\gamma_{BS} = 0.37$), and in Figure 10c, where the interfacial tension between the blocks and surfaces is increased ($\gamma_{AS} = 0.5$, $\gamma_{BS} = 0.58$) relative to the fixed $\gamma_{dp} = \gamma_{pS} = 0.3$. (As before, $N = 100$, $\gamma_{AB} = 1$, and $\Delta = 1.1L^*n$, where $n = 2$.)

Finally, in Figure 11, we plot the free energies for the parallel and perpendicular structures as a function of Δ for the case where $\phi_p = 0.15$, $R = 4$, $N = 100$, $\gamma_{AB} = 1$, $\gamma_{AS} = 0.3$, $\gamma_{BS} = 0.37$, and $\gamma_{pS} = \gamma_{dp} = 0.1$. The figure also shows the analogous curves for a melt of pure, confined diblocks; these curves were obtained from our model by setting $\phi_p = 0$. A careful comparison of the curves shows that regions wherein the perpendicular phase is stable are broader in the filled system than in the unfilled one (see insets in Figure 11). In other words, the particles extend the region of stability of the perpendicular phase.

Previous comparisons of the SCF and strong segregation scaling theories for pure, confined diblocks[15,28] show that for neutral surfaces it is only through the SCF approach that the free energy of the perpendicular structure lies strictly below the parallel one. This is due to the fact that the conformation of the chains near the walls is more accurately captured through the SCF model; in particular, the interfacial width broadens close to the wall in the case of the neutral walls.[15,21,28] Such broadening effects are not taken into account in the scaling model. These conclusions are also valid in our studies of the filled films. The scaling theory does not yield results analogous to the ones in Figure 2, where the free energy for perpendicular structure lies distinctly below the parallel morphology. Nonetheless, the

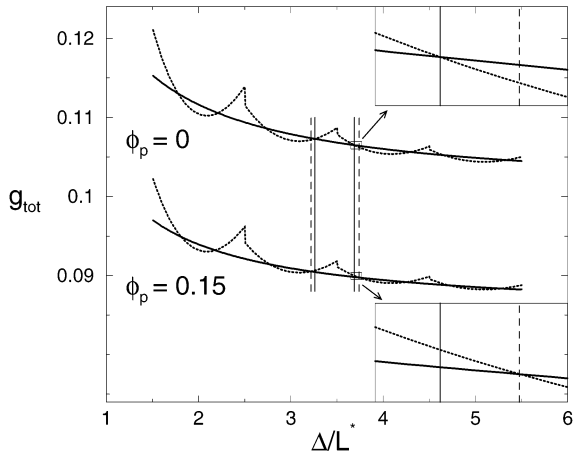

Figure 11. Free energy vs surface separation, Δ/L^*, in the cases of pure ($\phi_p = 0$) and filled ($\phi_p = 0.15$) diblocks for the parallel (dashed curves) and perpendicular (solid curves) structures. The results are calculated using the SST. Here, $N = 100$, $R = 4$, $\gamma_{AB} = 1$, $\gamma_{As} = 0.3$, $\gamma_{Bs} = 0.37$, and $\gamma_{dp} = \gamma_{ps} = 0.1$. The dashed vertical lines indicate a region of stability for the perpendicular phase in the case of the filled system, and the solid lines indicate the corresponding region of stability for the perpendicular phase in the case of the pure, unfilled system. Clearly, the region of stability for the filled system is broader than that for the unfilled melt. The insets show enlargements of the sections marked by squares in the plot.

above scaling results clearly indicate that the neutral particles localize near the surface layer and drive the system to self-assemble into the perpendicular phase.

Conclusions

Mixtures of polymers and nanoparticles can become highly frustrated when they are confined between hard walls. Both the conformational entropy of the chains and the translational entropy of the particles are compromised by the presence of the confining surfaces. Here, we used both the SCF/DFT approach and scaling theory to examine the behavior of these highly frustrated systems. We find that in such restricted geometries the constrained polymers essentially "push" the nanoparticles to the hard walls. If the particles are chemically distinct from the walls, they will effectively modify the chemical nature of this interface. This change in chemistry, in turn, affects the polymer−wall interactions and consequently the structure of the film.

We illustrate this point by considering two different examples of mixtures of nanoparticle and symmetric AB diblock copolymers. In the first example, we focus on *nonselective* or neutral particles and *selective* surfaces, which exhibit a preferential affinity for the A blocks. Using both the SCF/DFT and scaling approaches, we isolate a range of parameters for which neutral particles become localized at the selective walls. When the particle concentration at the walls is sufficiently high, the polymers switch orientation to form a surface-perpendicular lamellar structure. The neutral particles decorate the interfaces between the A/B domains. In effect, the confining walls have promoted the self-assembly of the system into particle nanowires that extend throughout the films and are separated by nanoscale stripes of polymer domains.

In the second example, we examined the case of diblocks and *selective* particles, which displayed an affinity for the A blocks, that are confined between two *nonselective* surfaces. Again, the particles are driven to the walls and modify the chemical nature of these surfaces. Now, however, the walls becomes more A-like, switching this surface from one that had a neutral interaction with both blocks to one that has a preferential interaction with the A phase. Confined between such selective surfaces, the optimal orientation of the film switches from surface perpendicular to surface parallel.

The results point to a novel technique for modifying the chemical nature of coatings and films entirely through self-assembly. This technique relies on an entropic effect, namely, the depletion attraction between the particles and walls. Entropically driven effects are relatively robust and can be applied more generally than approaches that rely primarily on chemistry-specific enthalpic effects. Thus, harnessing such entropic effects can prove to be useful in the fabrication of novel nanostructured materials[7,29] and coatings.

Finally, it is worth noting that particles near the top and bottom substrates can potentially enhance the wear properties of the films. If the substrates sustain damage, the underlying hard particles can, for example, prevent the propagation of a cracks into subsequent layers of the polymeric film. Thus, the addition of a small volume fraction of nanoparticles to confined polymer films can be advantageous in extending the lifetime of these coatings.

Acknowledgment. A.C.B. gratefully acknowledges the NSF, DOE, and ARO for financial support.

References and Notes

(1) Manne, S.; Aksay, I. *Curr. Opin. Solid State Mater. Sci.* **1997**, *2*, 358 and references therein.
(2) Kotov, N. *Mater. Res. Bull.* **2001**, *26*, 992 and references therein.
(3) Lu, Y.; et al. *Nature (London)* **2001**, *410*, 913.
(4) Decher, G. *Science* **1997**, *277*, 1232 and references therein.
(5) There is extensive research in this area; for a review of the relevant studies see: Fasolka, M. J.; Mayes, A. M. *Annu. Rev. Mater. Res.* **2001**, *31*, 323 and references therein.
(6) Thompson, R. B.; Ginzburg, V. V.; Matsen, M. W.; Balazs, A. C. *Science* **2001**, *292*, 2469.
(7) Lee, J. Y.; Thompson, R. B.; Jasnow, D.; Balazs, A. C. *Phys. Rev. Lett.* **2002**, *89*, 155503.
(8) Lee, J. Y.; Thompson, R. B.; Jasnow, D.; Balazs, A. C. *Macromolecules* **2002**, *35*, 4855.
(9) Thompson, R. B.; Lee, J. Y.; Jasnow, D.; Balazs, A. C. *Phys. Rev. E* **2002**, *66*, 031801.
(10) Lee, J. Y.; Thompson, R.; Jasnow, D.; Balazs, A. C. *J. Chem. Soc., Faraday Discuss.* **2003**, *123*, 121.
(11) Thompson, R. B.; Ginzburg, V. V.; Matsen, M. W.; Balazs, A. C. *Macromolecules* **2002**, *35*, 1060.
(12) At the size scales studied here, our SCF/DFT calculations show that there is no significant difference in the behavior of cubic and spherical particles when they are added to bulk diblocks. Our motivation for focusing on cubic particles is that the density functional theory for these fillers can be readily extended to parallelepipeds, and thus, we can investigate the effect of varying the particles' aspect ratio on the structure of the films. We also note that, in previous studies on the bulk properties of diblock/particle mixtures,[13] we compared our findings from Monte Carlo simulations with cubic particles to scaling theory with spherical particles and found that cubes and spheres of comparable sizes yield qualitatively similar behavior with regard to the structure of the system.
(13) Huh, J.; Ginzburg, V.; Balazs, A. C. *Macromolecules* **2000**, *33*, 8085.
(14) Shou, Z.; Buxton, G. A.; Balazs, A. C. *Compos. Interfaces* **2003**, *10*, 343.
(15) Matsen, M. W. *J. Chem. Phys.* **1997**, *106*, 7781.
(16) Cuesta, J. A.; Martinez-Raton, Y. *J. Chem. Phys.* **1997**, *107*, 6379.
(17) Drolet, F.; Fredrickson, G. H. *Phys. Rev. Lett.* **1999**, *83*, 4317.
(18) Bohbot-Raviv, Y.; Wang, Z.-G. *Phys. Rev. Lett.* **2000**, *85*, 3428.
(19) Turner, M. S. *Phys. Rev. Lett.* **1992**, *69*, 1788.

(20) Walton, D. G.; et al. *Macromolecules* **1994**, *27*, 6225.
(21) Pickett, G.; Balazs, A. C. *Macromolecules* **1997**, *30*, 3097.
(22) Carnahan, N. F.; Starling, K. E. *J. Chem. Phys.* **1969**, *51*, 635.
(23) Solis, F.; Tang, H. *Macromolecules* **1996**, *29*, 7953.
(24) Kellogg, G. J.; et al. *Phys. Rev. Lett.* **1996**, *76*, 2503.
(25) Jain, A.; Gutmann, J. S.; Garcia, C. B. W.; Zhang, Y. M.; Tate, M. W.; Gruner, S. M.; Wiesner, U. *Macromolecules* **2002**, *35*, 4862.
(26) The value of the $\gamma_{ij} \approx \sqrt{\chi}$. We chose a value of γ_{AB} that is sufficiently high so that the system is in the strong segregation regime, i.e., where $\chi N \gg 10.5$. We then chose the remaining $\gamma_{ij} < \gamma_{AB}$.
(27) In this scaling theory, we do not take into account the swelling of lamellar period in the particle-filled layers relative to the unfilled layers as the changes in the lamellar period are minor. We have observed in our SCF/DFT calculations approximately 4% degrease in the lamellar period with the addition of neutral fillers. Here, particles localized at the A/B interfaces act as compatibilizers.
(28) Geisinger, T.; Muller, M.; Binder, K. *J. Chem. Phys.* **1999**, *111*, 5241.
(29) Bockstaller, M. R.; Lapetnikov, Y.; Margel, S.; Thomas, E. L. *J. Am. Chem. Soc.* **2003**, *125*, 5276.

MA034765D